Supporting information

Rapid and reliable microfluidic blood typing based on laser identified RBC agglutination method

Bing Xu*[,a], Yange Huang[a], Shuqiang Min[a], Xianchang Wu[a], Tonghuan Zhan[a], Jiahao Liu[a], Fuzhou Niu*[,a], Hui Niu*[,b]

a School of Mechanical Engineering, Suzhou University of Science and Technology, Suzhou, 215009, China;

b Department of Pathology, The Second Affiliated Hospital of Soochow University, Suzhou, 215000, China;

E-mail: xb022@ustc.edu.cn & niu_hui513@163.com & fzniu@usts.edu.cn

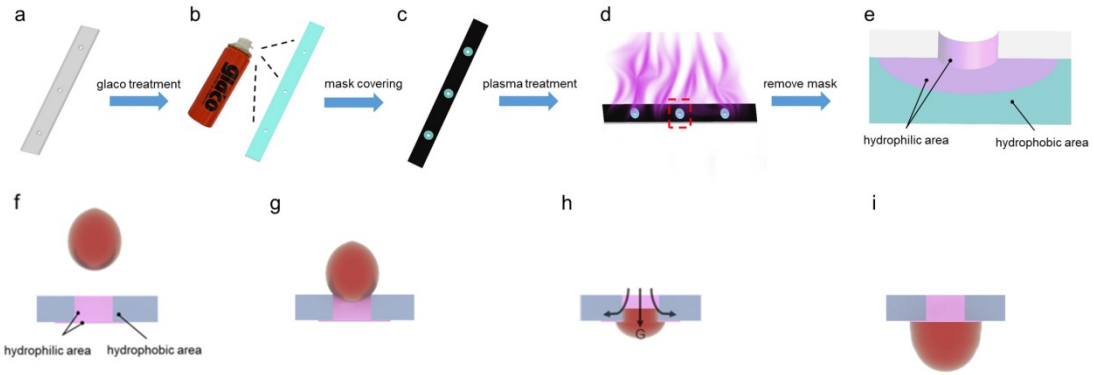

Fig. S1 Surface hydrophilicity treatment process for carrier plates. (a-b) The surface of the carrier plate was treated using a Glaco hydrophobic reagent. (c) One side of the carrier plate was covered using a mask with holes. (d) Hydrophilic treatment of the mask using a plasma machine. (e) The mask is removed and the final carrier plate with a fixed hydrophilic region is obtained. (f- i) Schematic diagram of introducing a droplet.

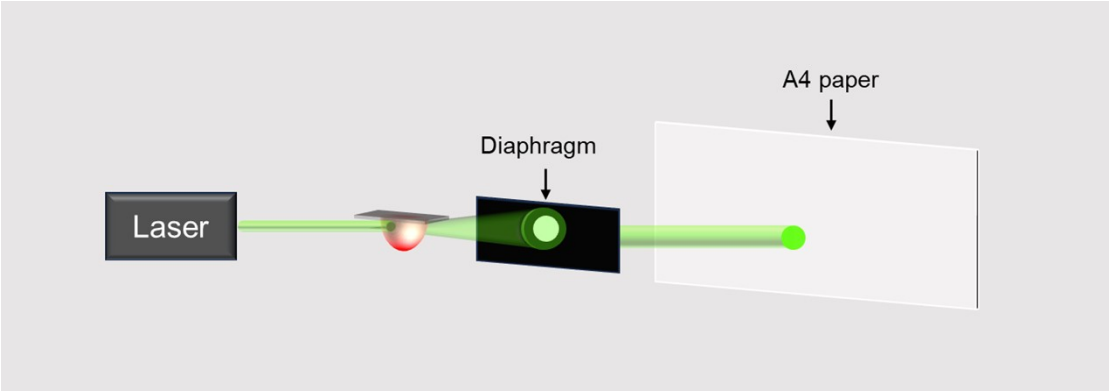

Fig. S2 Schematic diagram of laser penetration results.

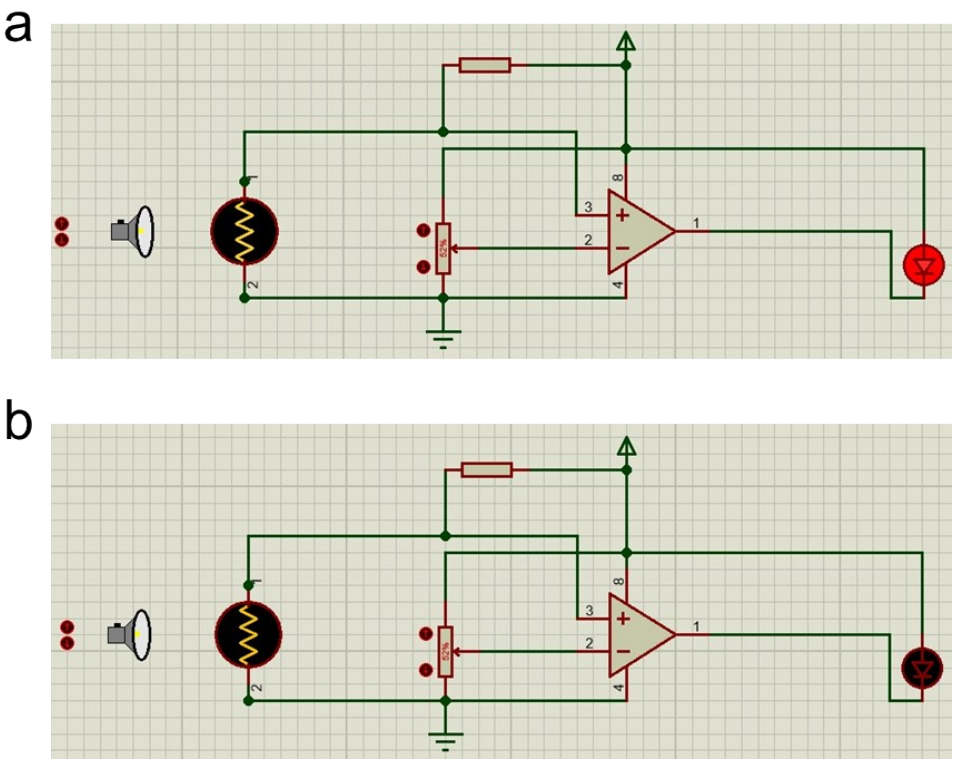

Fig. S3 Circuit simulation. (a) LEDs light up in high brightness conditions. (b) LED off in low brightness conditions.

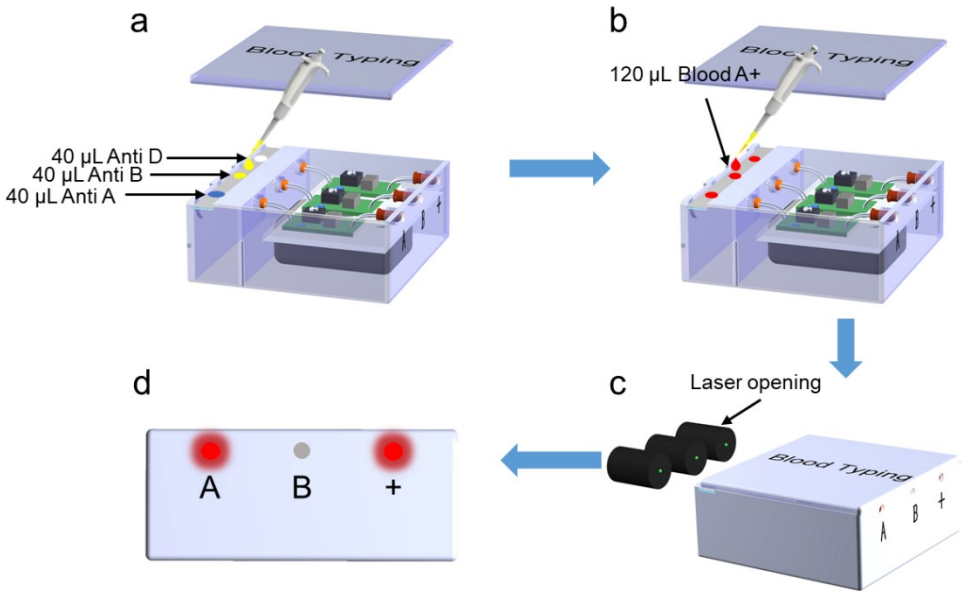

Fig. S4 Schematic diagram of the testing process. (a) The three antibodies (40 μL) were dropped into the three holes of the carrier plate. (b) Introducing the same volume of blood sample into the antibody. (c) Close the top cover to prevent the external light source from influencing the results, and wait for 5min. (d) Open the laser and observe the final result. For example, if an A+ blood sample is used, the result shows that the LEDs at “A” and “+” light on and the one at “B” lights off.

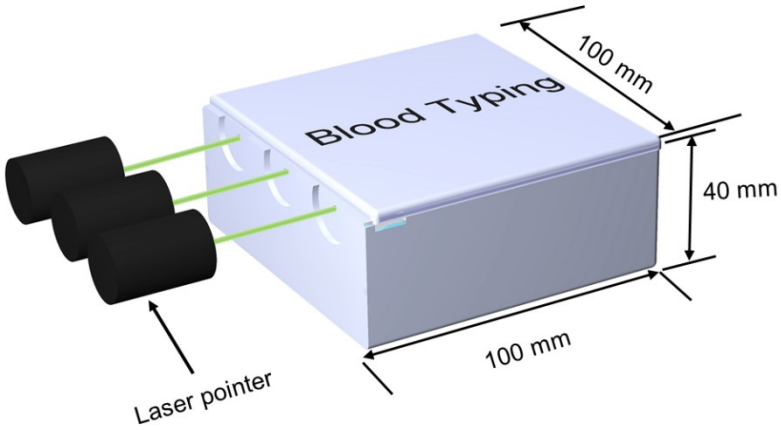

Fig. S5 Diagram of the dimensions of the laser-based blood typing device.

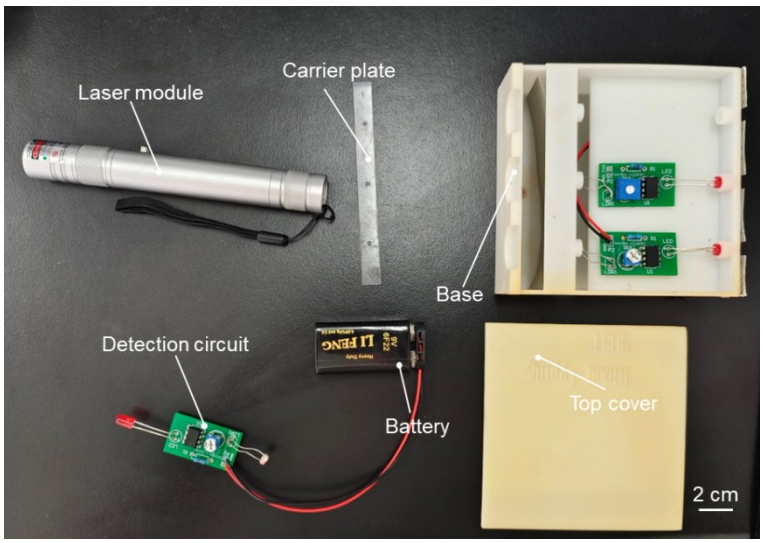

Fig. S6 The real image of the blood-typing device. The device consists of six parts, namely the top cover, detection circuit, sample carrier plate, laser module, battery, and base.

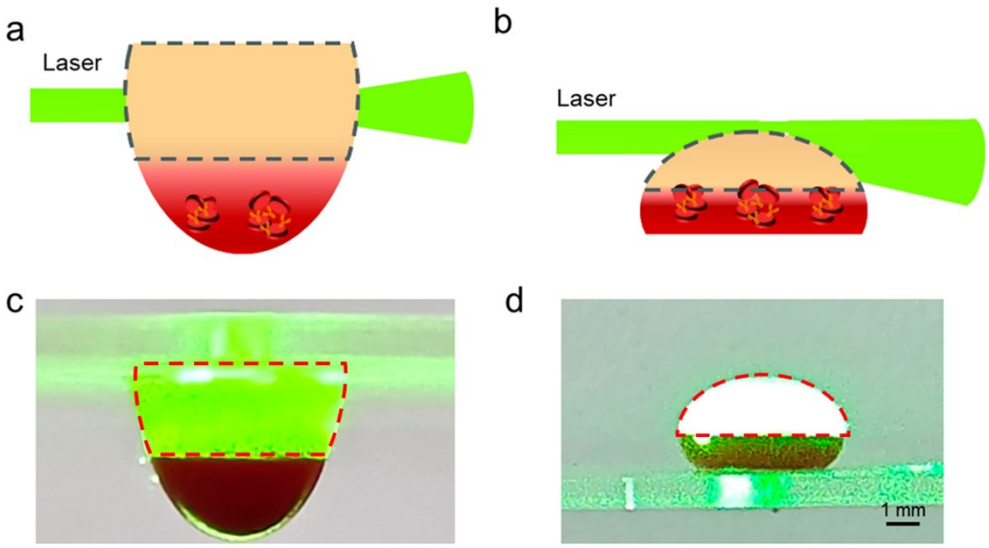

Fig. S7 The shape of the clarified layer of directly placed droplets and overhanging droplets. (a) Schematic of an overhanging droplet. (b) Schematic of a positively released droplet. (c) Optical image of an overhanging droplet. (d) Optical image of a positively released droplet.

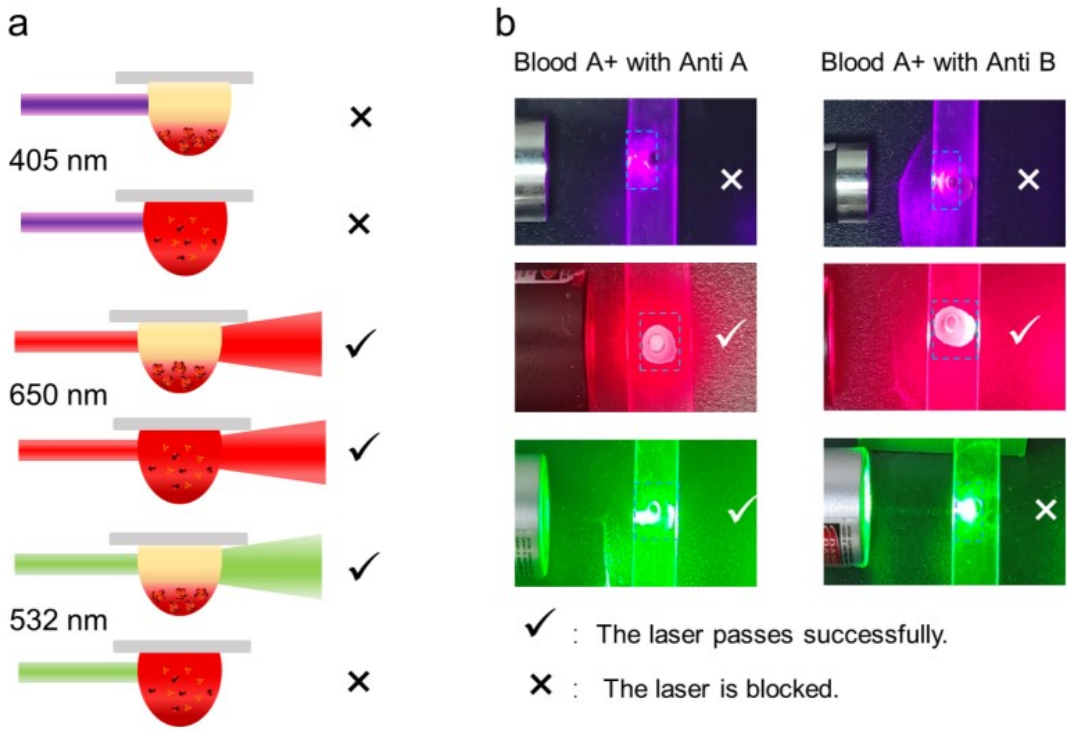

Fig. S8 (a) Schematic diagram of the transmission of the three different wavelengths of lasers. (b) Actual images of the transmission results of the three lasers. When 405 nm lasers illuminate the both samples, they are absorbed by the upper layer and cannot pass through. Once using a 650 nm red laser, it is found that the laser can pass through both positive and negative samples. Only the 532 nm green laser is able to transmit through the positive sample while being blocked by the negative sample.

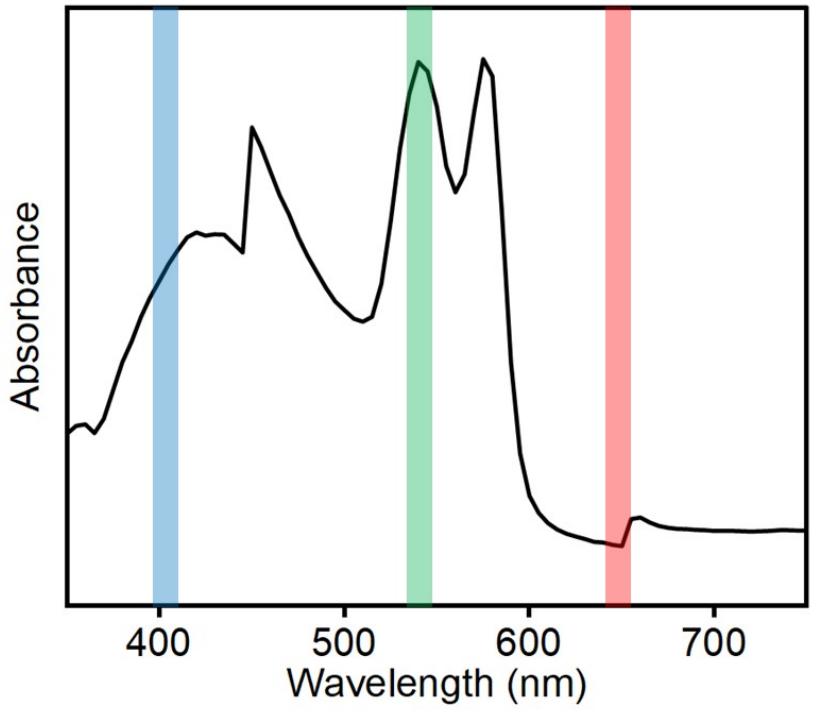

Fig. S9 Absorption spectra of diluted blood in the wavelength range from 350-750 nm. The blue and green lasers exhibit high absorption, thus preventing penetration into blood. In contrast, the red laser, with the lowest absorption, can readily penetrate the blood sample.

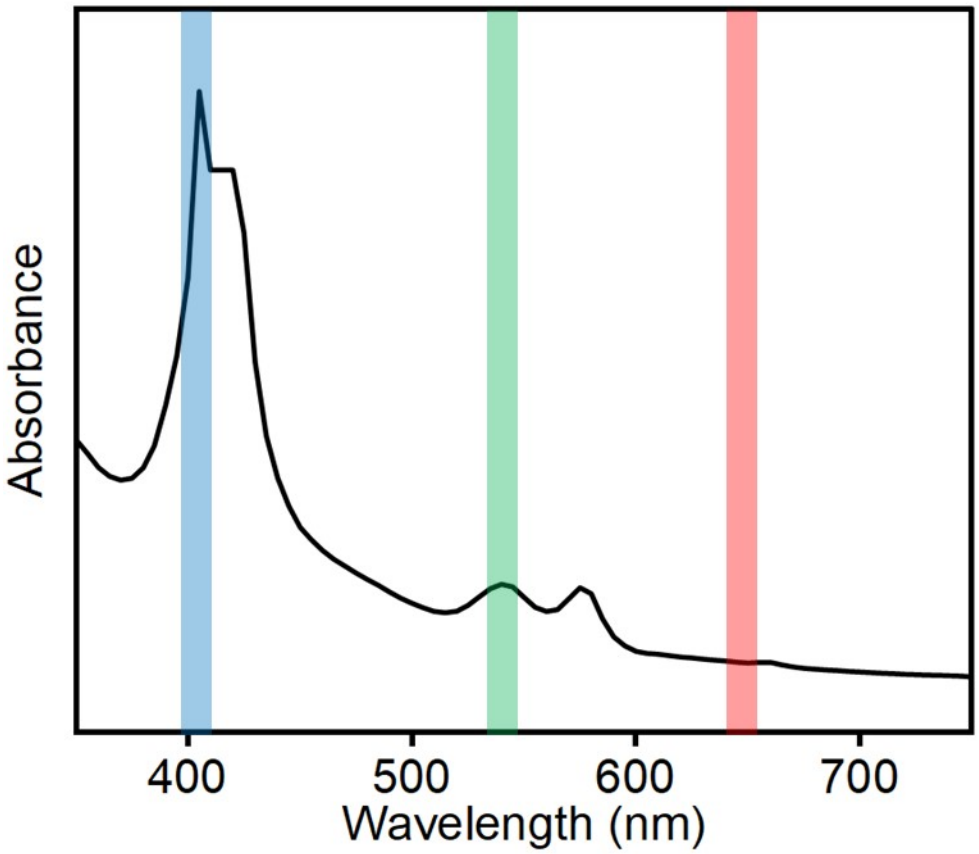

Fig. S10 Absorption spectra of plasma in the wavelength range from 350-750 nm. The blue laser exhibits the highest absorption, thus preventing penetration into plasma sample. In contrast, the red and green lasers, with the low absorption, can readily penetrate the plasma sample.

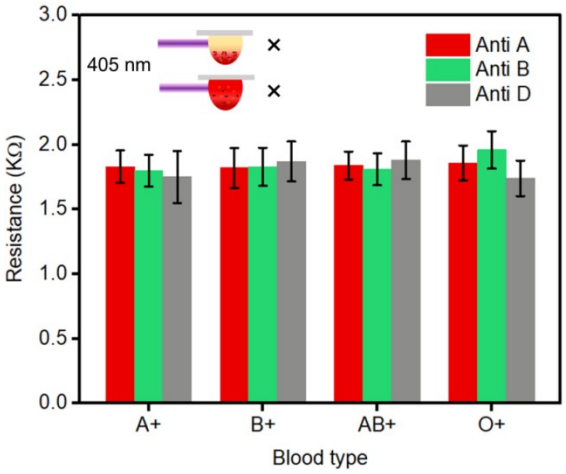

Fig. S11 The photoresistor resistance measurements when irradiating negative/positive samples using 405 nm violet lasers. It can be noticed that the photoresistors are always in high resistance state.

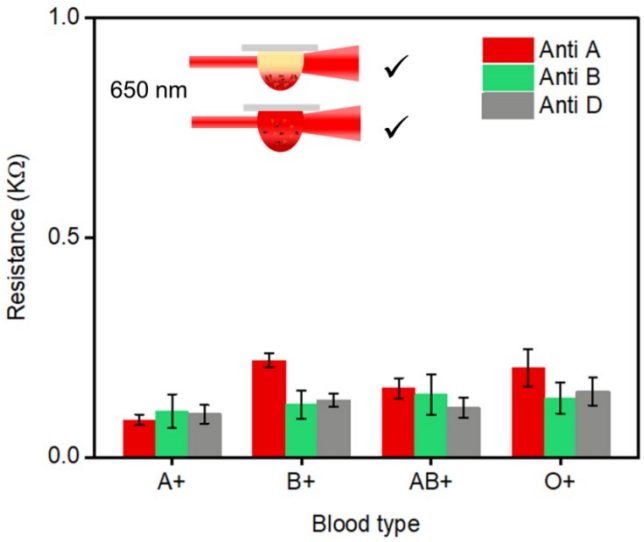

Fig. S12 Photoresistor resistance investigations when irradiating negative/positive samples using 650 nm red lasers. It can be noticed that the photoresistors are always in low resistance states.

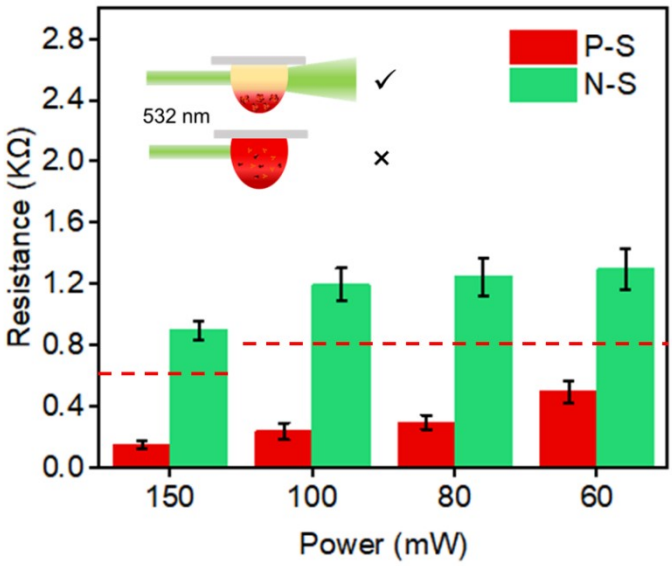

Fig. S13 Measurement of photoresistor resistance after different intensity of laser irradiation. Error bars indicate the standard deviation of the resistance values in different samples (N=6).

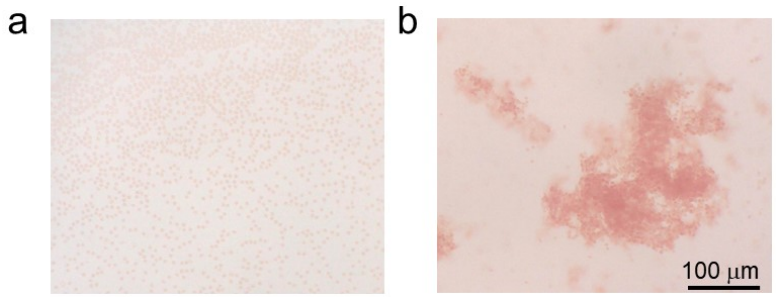

Fig. S14 (a) Optical image of RBCs after laser irradiation. (b) Optical image of RBC agglutination after laser irradiation.

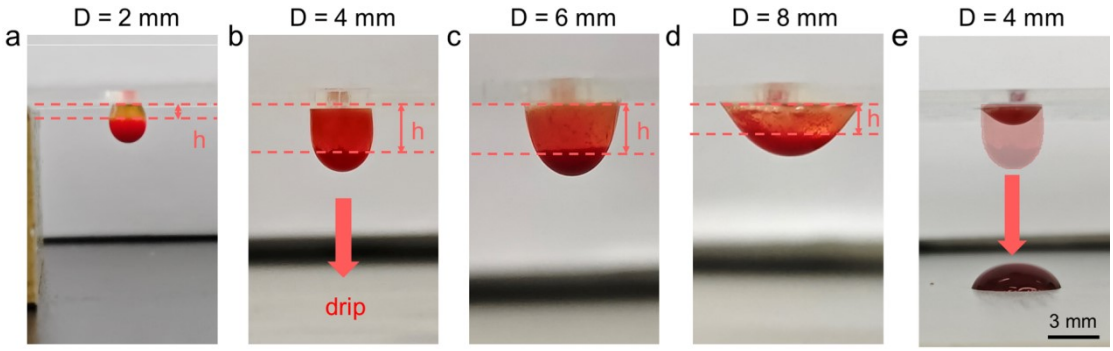

Fig. S15 Effect of different hydrophilic regions on carrying sample droplets. (a) The hydrophilic region with 2 mm diameter has a poor capacity to form droplets with a large CLH. (b) Hydrophilic regions with a diameter of 4 mm are able to form suspended droplets with a high CLH, but the droplets are less stable. (c) The hydrophilic region with 6 mm diameter enables the formation of stable and suspended droplets with a high CLH layer. (d) The hydrophilic region with 8 mm diameter is capable of carrying a large volume of samples, results in a low CLH. (e) A droplet falling from the hydrophilic region with a diameter of 4 mm.

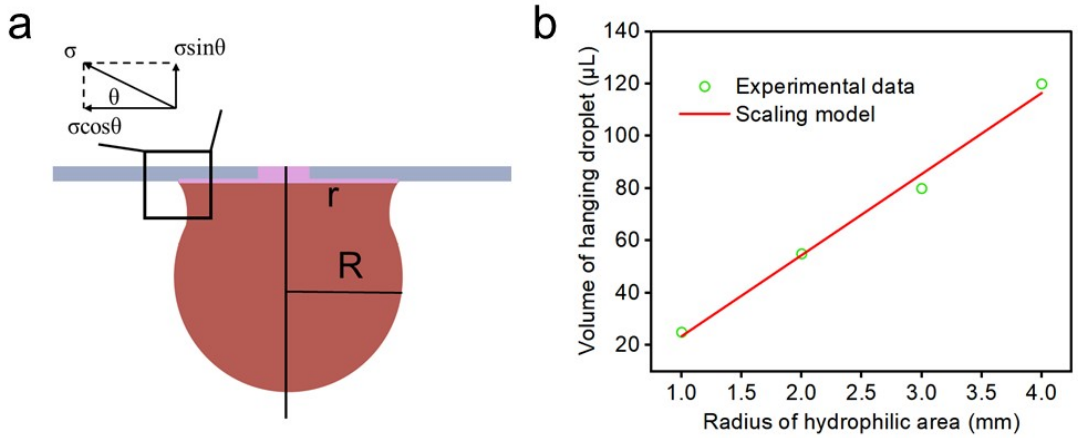

Fig. S16 (a) Mechanical analysis of suspended droplets on a horizontal carrier plate as the sample volume increases.

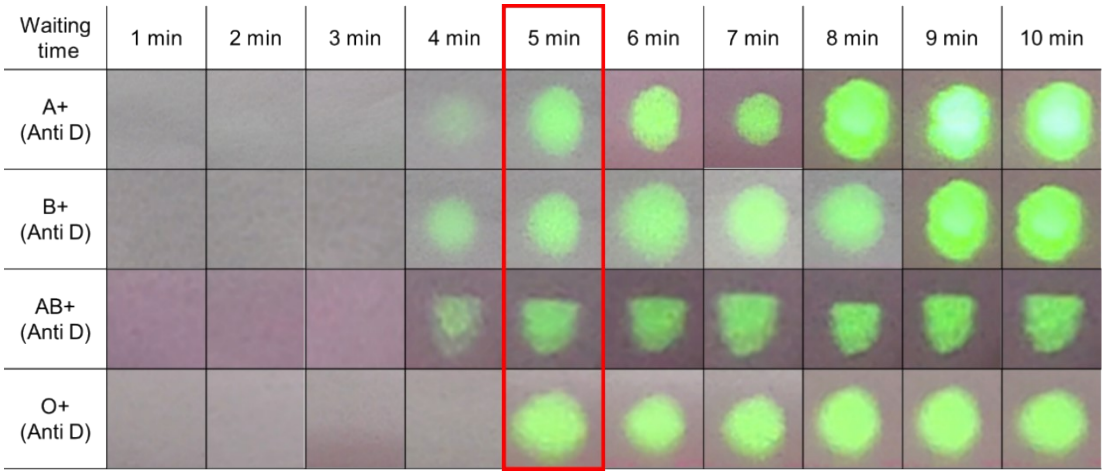

Fig. S17 Laser penetration results of different blood groups mixed with anti-D at different reaction times (1-10 minutes). The red rectangle box represents the laser penetration results at the optimum time.

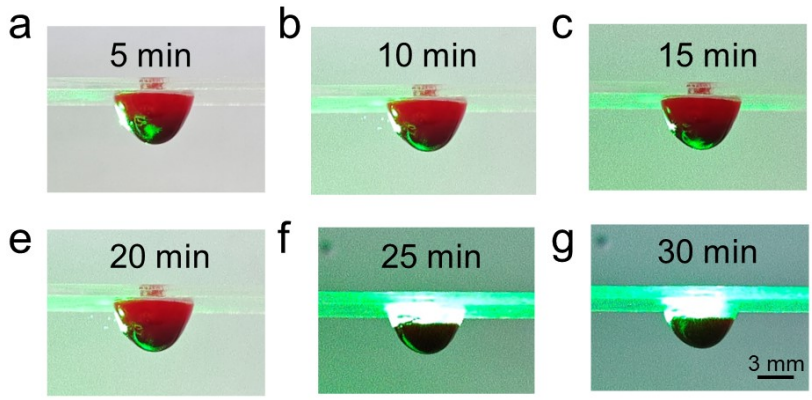

Fig. S18 Optical image of the sedimentation of A+ blood over 30 minutes. The laser is used to identify the delamination.

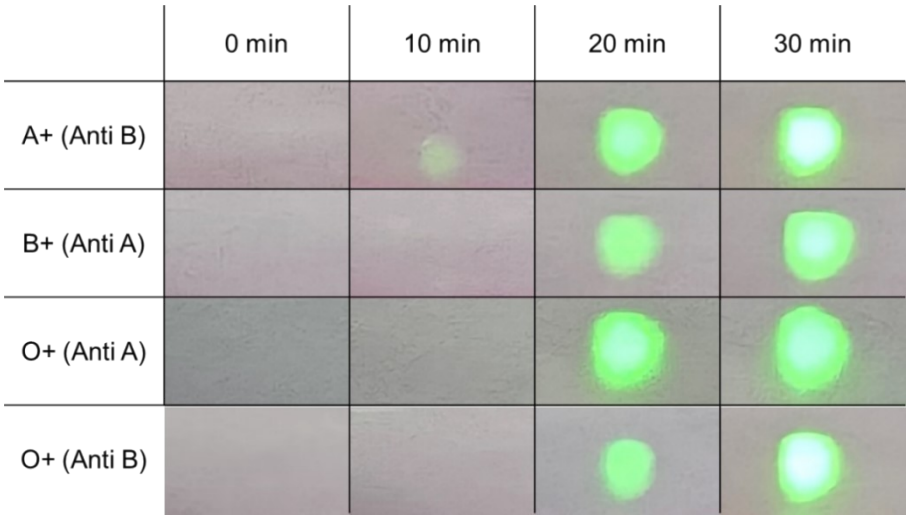

Fig. S19 Laser transmission results in negative samples with prolonged reaction times. It can be observed that excessively long reaction times can also lead to stratification of negative samples.

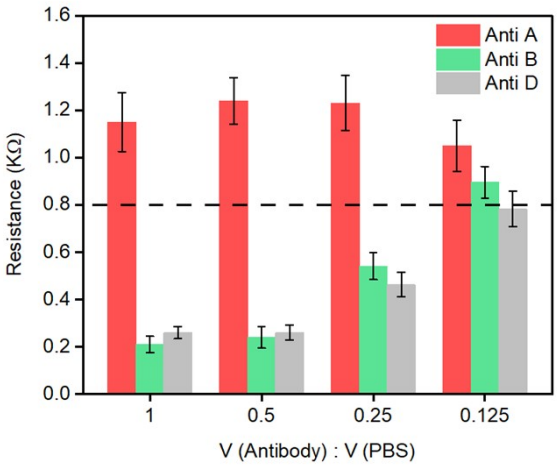

Fig. S20 The effect of different antibody dilutions on the resistor resistance (B+ blood). A good distinction between negative and positive samples can be made even at a fourfold dilution.

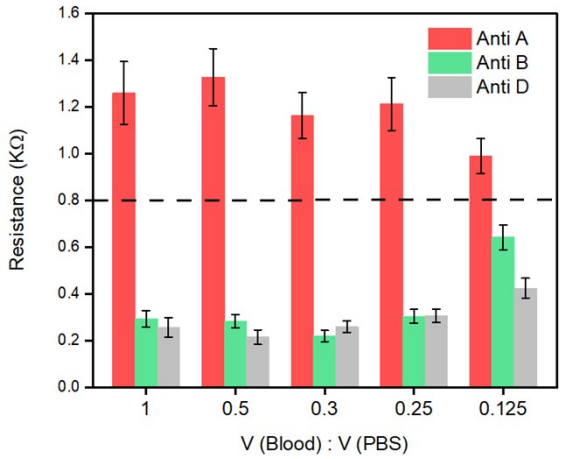

Fig. S21 The effect of different blood dilutions on the resistor resistances (B+ blood). It can be found that the dilution of eight times is still able to distinguish the negative and positive samples.

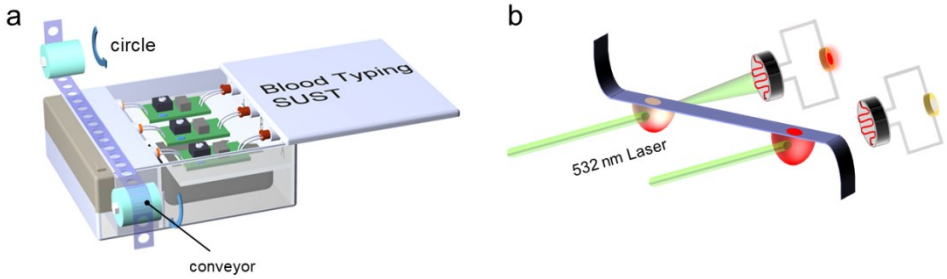

Fig. S22 Schematic diagram of large throughput blood-typing device.

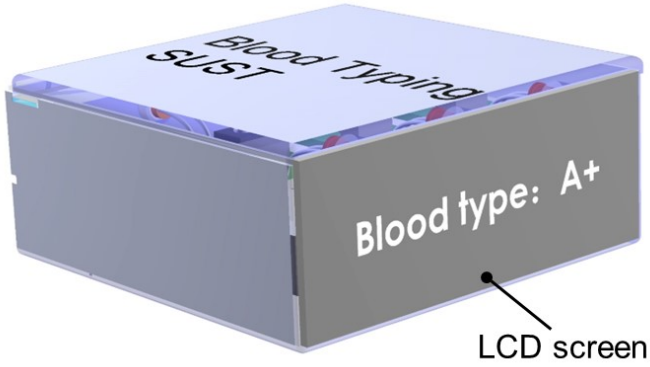

Fig. S23 Schematic of the blood typing result output from the LCD display.

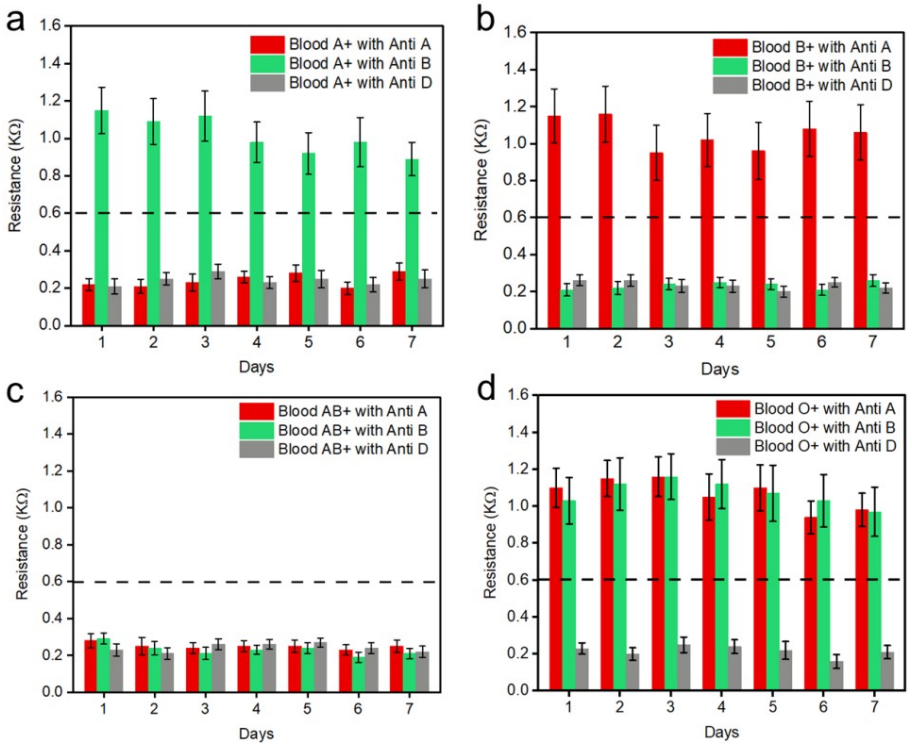

Fig. S24 Repeatability validation of blood-typing over seven days for four blood types. The device is found to have high detection stability within seven days.

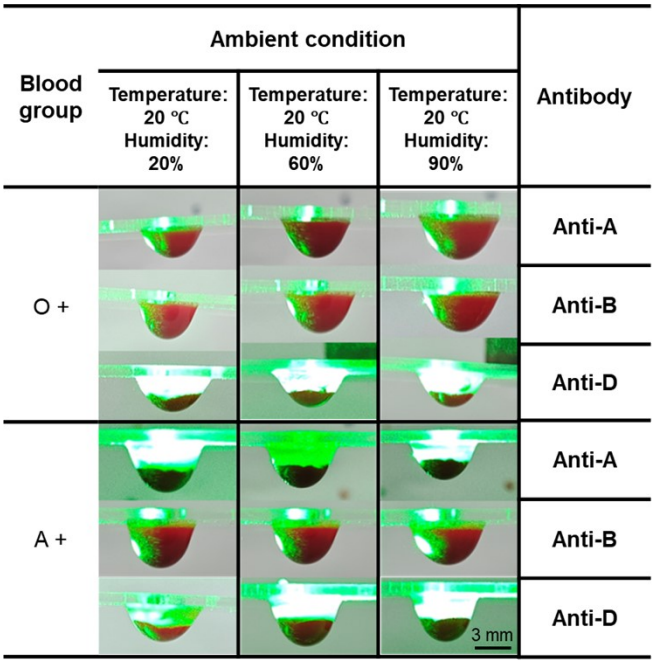

Fig. S25 The effect of different humidity levels on experiments.

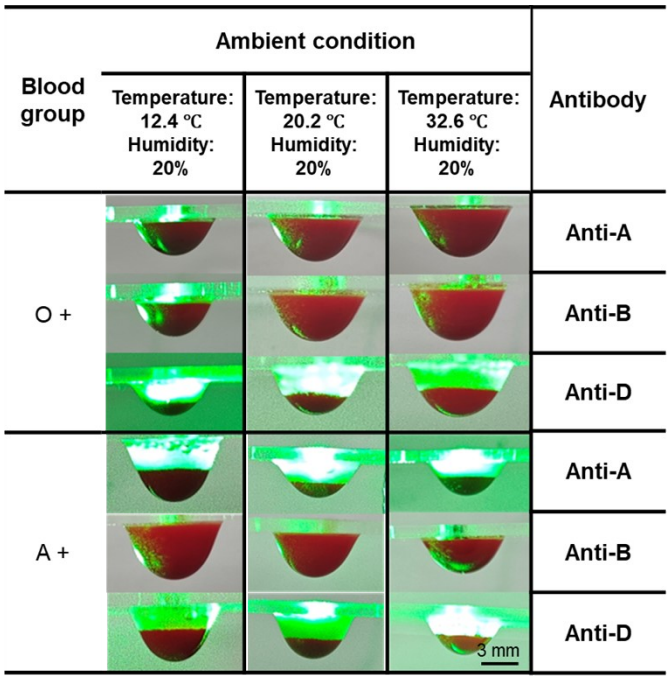

Fig. S26 The effect of different ambient temperatures on experiments.

Blood group	Light interference		
	Illumination: 50 Lux	Illumination: 300 Lux	Illumination: 800 Lux
A +	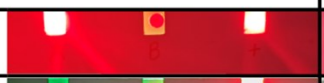	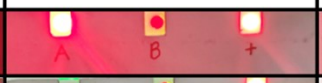	
O +	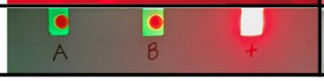	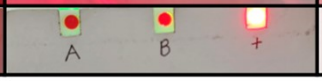	

Fig. S27 The effect of different light interference on experiments.

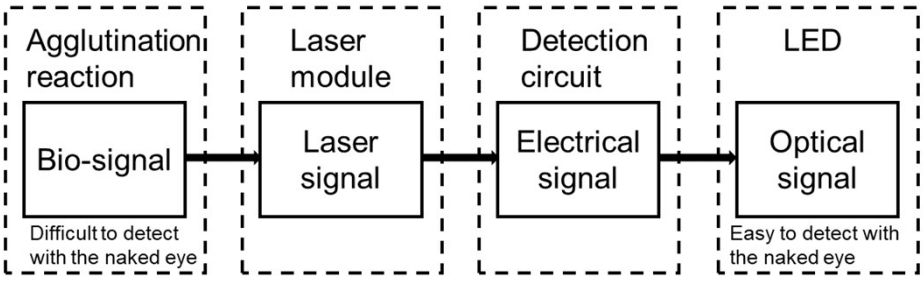

Fig. S28 Signal conversion flowchart.

Blood type		Antibody
A+	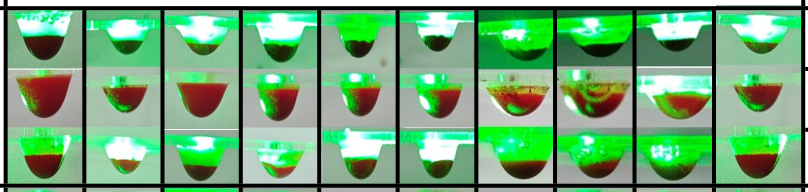	Anti-A
		Anti-B
		Anti-D
B+	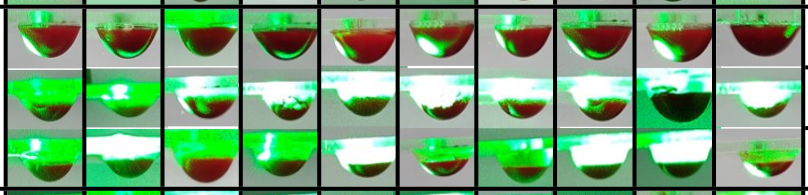	Anti-A
		Anti-B
		Anti-D
AB+	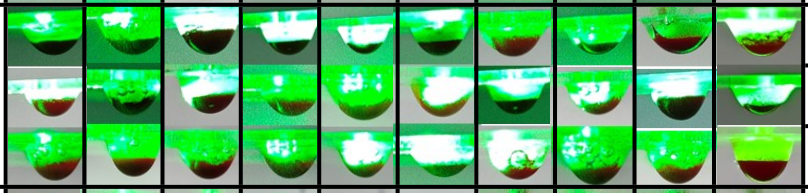	Anti-A
		Anti-B
		Anti-D
O+	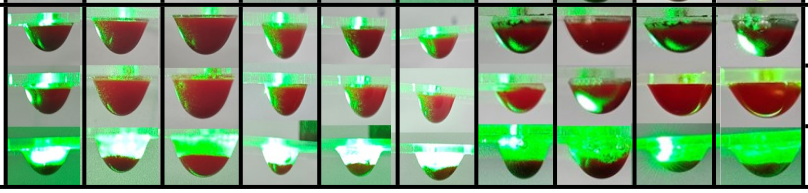	Anti-A
		Anti-B
		Anti-D

Table. S1 Summary of 40 blood-typing results by laser based-based methods.

Reference	Fabrication difficulty	Operation difficulty	Cost	Instrument cost	Price/test	Accuracy	Readability	Analysis time	Blood volumes	Resulting signal
ACS Nano 2021, 15, 7649−7658	Easy	Easy	High	-	-	100 %	High	2 min	120 μL	Optical signal
Clinical Chemistry 2021 67:12 1699–1708	Difficulty	Easy	High	$7000	$3	100 %	High	3 min	3 μL	Optical signal
Angew. Chem. Int. Ed. 2012, 51, 5497 – 5501	Easy	Difficulty	Low	-	$0.01	100 %	Low	2 min	60 μL	Bio-signal
Lab Chip, 2023, 23, 3272–3279	Difficulty	Difficulty	High	-	~$0.32	100 %	High	1 min	5 μL	Optical signal
Lab Chip, 2015, 15, 4533–4541	Difficulty	Easy	Low	-	-	100 %	Low	1 min	6 μL	Bio-signal
ORTHO VISION Analyzera	Difficulty	Difficulty	High	$137300	$1.58	100 %	High	-	-	Bio-signal
This work	Easy	Easy	Low	$3.23	$0.132	100 %	High	5 min	120 μL	Optical signal

Table S2. Comparison of different blood typing devices, of which our laser identification method of RBC agglutination reaction has the advantages of simplicity, low cost, easy-to-use and good readability. The cost includes instrument cost and test cost. The cost of the instrument consists of the detection circuit, the top cover, the base and the laser module, is $0.8, $1.48 and $0.48, respectively. The cost of the test ($0.132) is for the antibody.

	The price of top cover	The price of carrier plate	The price of detection circuit	The price of base	The price of battery	The price of laser module	The price of antibody solution	The total price
This work	0.44	0.03	0.8	1.07	0.41	0.48	0.132	3.362

Table S3. Detailed breakdown of component costs.

	Expected lifespan			Maintenance
This work	Power supply	Detection circuit	3d printed enclosure	1.Regular cleaning 2.Avoid storage in humid places 3.Regular battery replacement
	>1000 times	> 110000 h	> 120000 h	

Table. S4 Lifespan and maintenance information for blood typing devices.